

# AFG3L2 and ACO2-Linked Dominant Optic Atrophy: Genotype–Phenotype Characterization Compared to OPA1 Patients



GIULIA AMORE, MARTINA ROMAGNOLI, MICHELE CARBONELLI, MARIA LUCIA CASCAVILLA, ANNA MARIA DE NEGRI, ARTURO CARTA, VINCENZO PARISI, ANTONIO DI RENZO, COSTANTINO SCHIAVI, CHIARA LENZETTI, CORRADO ZENESINI, DANARA ORMANBEKOVA, FLAVIA PALOMBO, CLAUDIO FIORINI, LEONARDO CAPORALI, VALERIO CARELLI, PIERO BARBONI, AND CHIARA LA MORGIA

• **PURPOSE:** Heterozygous mutations in the AFG3L2 gene (encoding a mitochondrial protease indirectly reflecting on OPA1 cleavage) and ACO2 gene (encoding the mitochondrial enzyme aconitase) are associated with isolated forms of Dominant Optic Atrophy (DOA). We aimed at describing their neuro-ophthalmological phenotype as compared with classic OPA1-related DOA.

• **DESIGN:** Cross-sectional study.

• **METHODS:** The following neuro-ophthalmological parameters were collected: logMAR visual acuity (VA), color vision, mean deviation and foveal threshold at visual fields, average and sectorial retinal nerve fiber layer (RNFL), and ganglion cell layer (GCL) thickness on optical coherence tomography. ACO2 and AFG3L2 patients were compared with an age- and sex-matched group of OPA1 patients with a 1:2 ratio. All eyes were analyzed using a clustered Wilcoxon rank sum test with the Rosner–Glynn–Lee method.

• **RESULTS:** A total of 44 eyes from 23 ACO2 patients and 26 eyes from 13 AFG3L2 patients were compared with 143 eyes from 72 OPA1 patients. All cases presented with bilateral temporal-predominant optic atrophy with various degree of visual impairment. Comparison between AFG3L2 and OPA1 failed to reveal any significant difference. ACO2 patients compared to both

AFG3L2 and OPA1 presented overall higher values of nasal RNFL thickness ( $P = .029$ ,  $P = .023$ ), average thickness ( $P = .012$ ,  $P = .0007$ ), and sectorial GCL thickness. These results were confirmed also comparing separately affected and subclinical patients.

• **CONCLUSIONS:** Clinically, DOA remains a fairly homogeneous entity despite the growing genetic heterogeneity. ACO2 seems to be associated with an overall better preservation of retinal ganglion cells, probably depending on the different pathogenic mechanism involving mtDNA maintenance, as opposed to AFG3L2, which is involved in OPA1 processing and is virtually indistinguishable from classic OPA1-DOA. (Am J Ophthalmol 2024;262: 114–124. © 2024 The Authors. Published by Elsevier Inc. This is an open access article under the CC BY license (<http://creativecommons.org/licenses/by/4.0/>))

**D**OMINANT OPTIC ATROPHY (DOA) IS AN autosomal dominant inherited condition caused by loss of retinal ganglion cells (RGCs). Insidious central visual loss or inability to reach full vision at ophthalmic evaluations is usually recognized in the first 2 decades of life, frequently with a positive family history for low vision even if disease penetrance and clinical expression vary considerably among relatives.<sup>1</sup> Although optic atrophy is usually the only clinical feature, DOA may be associated with other neurological signs such as hearing loss, ptosis, and chronic progressive external ophthalmoplegia (CPEO) with myopathy, peripheral neuropathy, and other rare manifestations such as parkinsonism, dementia, or multiple sclerosis, a condition overall referred to as DOA-*plus*.<sup>2,3</sup>

About 60% of cases are due to heterozygous pathogenic variants in the OPA1 gene,<sup>4,5</sup> which encodes for an inner mitochondrial membrane (IMM) protein processed in multiple isoforms fulfilling several functions within the cell, primarily fusion of IMM and shaping of cristae morphology, but also tuning efficiency of OXPHOS and energy metabolism, apoptosis control, calcium handling, and maintenance of the mitochondrial genome (mtDNA)

 Supplemental Material available at [AJO.com](http://AJO.com).

Accepted for publication January 10, 2024.

From the Department of Biomedical and Neuromotor Sciences (G.A., M.C., V.C., C.L.M.), University of Bologna, Bologna, Italy; Ophthalmology Unit (G.A., C.S.), IRCCS Azienda Ospedaliero-Universitaria di Bologna, Bologna, Italy; IRCCS Istituto delle Scienze Neurologiche di Bologna (M.R., D.O., F.P., C.F.L.C.V.C.), Programma di Neurogenetica, Bologna, Italy; Department of Ophthalmology (M.L.C., P.B.), University Vita-Salute, IRCCS Ospedale San Raffaele, Milan, Italy; Azienda Ospedaliera San Camillo-Forlanini (A.M.D.N.), Rome, Italy; Ophthalmology Unit (A.C.), University Hospital of Parma, University of Parma, Parma, Italy; IRCCS Fondazione Bietti (V.P. A.D.R.), Rome, Italy; Department of Surgery and Translational Medicine (C.L.), Eye Clinic, Careggi University Hospital, University of Florence, Florence, Italy; IRCCS Istituto delle Scienze Neurologiche di Bologna (C.Z.), Unità di Epidemiologia e Statistica, Bologna, Italy; IRCCS Istituto delle Scienze Neurologiche di Bologna (C.L.M.), UOC Clinica Neurologica, Bologna, Italy. Inquiries to Giulia Amore, Università di Bologna, IRCCS Azienda Ospedaliero-Universitaria di Bologna, Bologna, Italy; e-mail: [giulia.amore4@unibo.it](mailto:giulia.amore4@unibo.it)

integrity.<sup>6</sup> Interestingly, at the opposite end of mitochondrial dynamics, also defective fission as due to mutations in the *DNM1L/DRP1* gene may lead to DOA in a minority of cases (OPA5),<sup>7</sup> pointing to balance between fusion and fission as a key mechanism for RGC survival and optic nerve physiology.<sup>8</sup>

Another gene (*OPA3*) and 2 further loci (*OPA4*, *OPA8*) are known to be associated with DOA, while additional loci and genes (*OPA2*, *OPA6*, *OPA7/TMEM126A*) are responsible for X-linked or recessive forms of optic atrophy.<sup>9</sup> Currently, the list of genes associated with DOA is undergoing rapid growth, thanks to the systematic use of whole exome sequencing (WES) and whole genome sequencing (WGS),<sup>9</sup> and it was recently enriched by the relatively frequent identification of pathogenic variants in *AFG3L2* (MIM# 604581)<sup>10–13</sup> and *ACO2* genes.<sup>14</sup> Other rare genetic causes of DOA are pathogenic variants in *SSBP1*<sup>15–17</sup> and *SDHA* genes.<sup>18</sup>

The *AFG3L2* gene encodes for a mitochondrial protease, which, in combination with paraplegin encoded by the *SPG7* gene, forms a mitochondrial matrix AAA metalloprotease (m-AAA), a proteolytic complex located in the IMM responsible for quality control and processing of several mitochondrial proteins, reflecting also on *OPA1* processing.<sup>19</sup> Mutations in *AFG3L2* were originally described to cause a dominant form of spinocerebellar ataxia (SCA28, MIM# 610246),<sup>20</sup> whereas homozygous mutations have been associated with a recessive spastic ataxia syndrome (SPAX5, MIM# 614487).<sup>21</sup> In recent years, heterozygous mutations in this gene have been increasingly recognized to cause non-syndromic DOA.<sup>10–13</sup> Remarkably, the SCA28-associated mutations affect the proteolytic domain, whereas all DOA-associated *AFG3L2* mutations cluster in the ATPase domain.<sup>12</sup> The pathogenic role of DOA-associated *AFG3L2* mutations was confirmed in yeast and in patients' fibroblasts, leading to the interesting observation of abnormal accumulation of short isoforms of *OPA1* skewing mitochondrial dynamics toward fission of mitochondria, with consequent fragmentation of the mitochondrial network.<sup>12,22</sup> Interestingly, recessive pathogenic mutations in the *SPG7* gene were associated with spastic paraparesis, either pure or associated with optic atrophy,<sup>23</sup> and, not surprisingly also for this gene, dominant mutations associated with DOA have been reported.<sup>13,24</sup>

Dominant mutations in another mitochondrial gene *ACO2*, encoding for the tricarboxylic acid-cycle enzyme aconitase, have been recently described to be a frequent cause of DOA.<sup>14,25</sup> Recessive mutations in *ACO2* have been previously associated with two distinct and severe infantile disorders: infantile cerebellar-retinal degeneration (ICRD; OMIM #614599) and optic atrophy 9 (OPA9; OMIM #616289).<sup>26</sup> Monoallelic mutation in *ACO2*-mutant fibroblasts have been demonstrated to be sufficient to cause mitochondrial respiration dysfunction and mtDNA depletion, leading to an increase in susceptibility to oxidative stress and cell death.<sup>27</sup>

In the present study, we aimed at characterizing the neuro-ophthalmological phenotype of patients with *AFG3L2* and *ACO2*-associated DOA, in comparison to patients with classical *OPA1*-DOA, highlighting, if any, the different genotype–phenotype correlations.

---

## METHODS

• **COHORT STUDY AND NEURO-OPHTHALMOLOGICAL ASSESSMENT:** In our cross-sectional study, after the approval of the Institutional Review Board (121-2019-OSS-AUSLBO-19012), we retrospectively investigated a cohort of patients with non-syndromic optic atrophy meeting the diagnostic criteria for DOA harboring heterozygous (monoallelic) mutations in *AFG3L2* or *ACO2* genes (Supplemental Tables 1 and 2). Patients followed at our Neuro-ophthalmological Clinic or referred to our Program of Neurogenetics for genetic diagnosis at IRCCS Istituto delle Scienze Neurologiche di Bologna (Ospedale Bellaria, Bologna, Italy) were included and signed the approved informed consent.

Information about family history and other symptoms were recorded. Given the insidious presentation of DOA, age at first evidence of optic disc atrophy was categorized into 3 groups: preschool (<6 years), childhood–adolescence (6–18 years), and adulthood (>18 years). Data retrieved from neuro-ophthalmological examination included the following: visual acuity (VA) converted into logMAR, color vision (Ishihara test), optic nerve appearance at slitlamp examination/fundus picture assessed by at least 2 different ophthalmologists or on 2 subsequent visits, computerized visual fields (VFs) (Humphrey Field Analyzer, protocol Sita Standard 30-2, Zeiss), optic nerve head (ONH) area, retinal nerve fiber layer (RNFL) thickness, and ganglion cell and plexiform layer (GCL) thickness assessed by optical coherence tomography (OCT) (DRI Triton, Topcon).<sup>28</sup>

We included patients with vision loss defined as logMAR >0, from now on referred to as affected/symptomatic, as well as patients with normal VA defined as logMAR <0 but displaying fundoscopic or instrumental signs of disease (temporal pallor or reduced RNFL thickness on OCT or both), from now on referred to as subclinical. Patients with myopia higher than 3 diopters (D) or astigmatism higher than 2 D were excluded. Eyes with significant ophthalmological conditions that could hamper the neuro-ophthalmological parameters (such as severe amblyopia or media opacities, maculopathy, or retinopathy) other than hereditary optic neuropathy were excluded. Relatives harboring a pathogenic mutation without any sign of visual involvement, clinical or instrumental, were also excluded.

Neuro-ophthalmological data were compared with data from group of *OPA1*-related DOA patients followed regularly at our Neuro-ophthalmological Clinic at IRCCS

Istituto delle Scienze Neurologiche di Bologna (Ospedale Bellaria, Bologna, Italy). We retrospectively retrieved neuro-ophthalmological data from the last available visit of patients carrying a heterozygous mutation in the *OPA1* gene (Supplemental Tables 1 and 2). We included patients followed from 2018 who had comparable OCT measures, both affected and subclinical patients displaying instrumental signs of disease. The same ophthalmological exclusion criteria were applied. Information about mutation type, family history, disease onset, and other symptoms were also recorded. Patients carrying a mutation in the *OPA1* gene were matched by age and sex with a 2:1 ratio, with patients carrying a mutation in the *AFG3L2* or *ACO2* gene to reduce the confounding effect of age and sex in group comparisons. Patients in the 3 groups were further classified according to type of mutation, namely missense or predicted to lead to loss of function (LoF), thus including small indels leading to frameshift, nonsense introducing stop codons, or variants in the splice regions.

During the past two decades, we used different genetic approaches to screen DOA patients. In Supplemental Table 1, we report on the method used to identify the pathogenic variant causing DOA in the family proband. Briefly, variants were identified by direct sequencing of *OPA1* or *ACO2* using specific primers in the families listed as “Sanger”; by SALSA MLPA Probemix P229 *OPA1* (MRC Holland) following the manufacturer’s instructions in the families listed as “MLPA”; by a next generation sequencing (NGS) targeted gene panel including 35 genes associated with hereditary optic neuropathy (HON) in the families listed as “HON Panel”; and by whole exome sequencing (WES), applying Nextera Rapid Capture Exome (Illumina) or xGen Exome Hyb Panel (Integrated DNA Technologies), in the families listed as “WES.”

- **STATISTICAL ANALYSIS:** The 3 patient groups (from now on referred as *AFG3L2*, *ACO2*, and *OPA1*) were analyzed to compare sex, age, mutation distribution, and visual function outcomes.

For each group, continuous variables were summarized with statistics including the number of patients (n), mean, SD, median, interquartile range (IQR). Shapiro–Wilk and Kolmogorov–Smirnov normality tests were used to assess the normal distribution of data. Demographic data were compared using univariate analysis of variance with a least significant difference post hoc test if normally distributed; otherwise the Kruskal–Wallis test was used, followed by the Dunn–Bonferroni post hoc test.

The following visual endpoints were analyzed: VA, mean deviation (MD), and fovea at VF, Ishihara color vision testing, ONH size, RNFL (average, temporal, superior, nasal, and inferior quadrants), and GCL (average and 6 individual macular sectors: supero-temporal, superior, supero-nasal, infero-nasal, inferior, and infero-temporal) thickness.

Primary statistical analysis was conducted for the aforementioned visual endpoints to compare the 3 patient

groups by applying a clustered Wilcoxon rank sum test (Rosner–Glynn–Lee method), and the Benjamini–Hochberg method was applied to adjust *P* values for multiple comparisons.<sup>29</sup> In particular, comparison among the 3 groups was conducted first on all patients, then only on patients with clear visual dysfunction (reduced visual acuity defined as logMAR >0). Separately, patients with normal VA but fundoscopic or instrumental signs of disease were also compared.

Secondary statistical analysis was performed in the same manner as the primary one with a clustered Wilcoxon rank sum test on the aforementioned visual endpoints by stratifying each group of patients (*AFG3L2/ACO2/OPA1*) by sex (male vs female) and mutation type (missense vs LoF) to identify any specific mutation type genotype–phenotype correlation. Given the exploratory nature of these secondary subgroup analyses, no adjustments for multiplicity were applied.

Two-sided *P* values are presented. Statistical analyses were carried out using R software, version 4.0.0, and IBM SPSS Statistics for Windows, version 20.0 (IBM Corporation) software.

---

## RESULTS

Demographic and general clinical/genetic features of the cohorts are shown in Table 1.

A total of 13 *AFG3L2* patients (9 male) belonging to 6 pedigrees (reported in Caporali et al.<sup>12</sup>) and 23 *ACO2* patients (17 male) from 15 families (some reported in Charif et al.<sup>14</sup>), were enrolled. Mean age was  $36.5 \pm 20.2$  years for *AFG3L2* patients and  $34.7 \pm 16.9$  years for *ACO2* patients. Neuro-ophthalmological data of 72 matched *OPA1* patients (mean age  $36.21 \pm 17.4$  years, 50 male) were retrieved and compared. As results of the matching procedure, age and sex were similarly distributed among the 3 groups: the *P* values were respectively .93 and .92 (Table 1).

Overall, a total of 91 affected patients (63 *OPA1*, 17 *ACO2*, and 11 *AFG3L2*) and 17 subclinical patients (9 *OPA1*, 6 *ACO2*, and 2 *AFG3L2*) were included in the study.

Among the affected patients, we found a similar age distribution of first evidence of optic disc atrophy in the 3 groups, with a higher prevalence of onset in childhood/adolescence in all 3 groups (Table 1). The number of affected relatives was not statistically different among groups (Table 1). Apart from optic atrophy, other neurological symptoms, either isolated or combined, were present in 23 patients (16 *OPA1*, 3 *ACO2*, and 4 *AFG3L2*). Noticeably, a higher rate of extraocular symptoms was observed in both *AFG3L2* and *OPA1* patients compared to *ACO2* patients (Table 1).

All *AFG3L2* patients presented missense mutations affecting the ATP-ase domain, as previously reported,<sup>12</sup>

**TABLE 1.** Cohort Description

	ACO2	AFG3L2	OPA1	P Value
Patients, n	23	13	72	
Age, y, mean ± SD (median)	34.7 ± 16.9 (32)	36.5 ± 20.2 (33)	36.2 ± 17.4 (35)	.93 <sup>a</sup>
Sex, male, n (%)	17 (73%)	9 (70%)	50 (70%)	.92 <sup>b</sup>
Mutation				
Missense, n (%)	13 (56%)	13 (100%)	14 (20%)	
Loss of Function, n (%)	10 (44%)	0	58 (80%)	
Status				
Subclinical, n (%)	6 (26%)	2 (15%)	9 (13%)	
Affected, n (%)	17 (74%)	11 <sup>c</sup> (85%)	63 (87%)	.29 <sup>b</sup>
Preschool onset (<6 y), n (%)	4 (23%)	2 (25%)	18 (29%)	.81 <sup>b</sup>
Childhood–adolescence onset, n (%)	11 (65%)	4 (50%)	31 (49%)	
Adulthood onset (> 18 y), n (%)	2 (12%)	2 (25%)	14 (22%)	
No. of affected relatives, mean ± SD	1.1 ± 0.9	2 ± 1.3	2.26 ± 2.4	.11 <sup>a</sup>
Other Neurological Symptoms, n (%)	3 (13%)	4 (30%)	16 (25%)	.24 <sup>b</sup>
Hearing loss	0	2	5	
Movement disorder	1	1	2	
Cognitive/psychiatric	1	2	4	
Migraine	1	0	3	
Myopathy/ptosis	0	0	2	

n = Absolute frequency; % =relative frequency.

<sup>a</sup>P value based on Kruskal–Wallis test.

<sup>b</sup>P value based on  $\chi^2$  test.

<sup>c</sup>Missing data (onset not available in 3 affected AFG3L2 patients).

whereas the ACO2 patients harbored a missense mutation in 56% of cases and other genetic defects predicted to cause LoF in the remaining 44% of cases. Patients with OPA1 mutations were also classified according to mutation type, distinguishing those predicted to cause LoF (n = 58, 80%) or missense (n = 14, 20%), with the awareness that in the large majority of cases, the latter variants are assumed to act as dominant negative, but not excluding the possibility that some of them may still lead to haploinsufficiency by destabilizing the protein product, as we have previously shown.<sup>3</sup> All mutations are listed in Supplemental Table 1.

Neuro-ophthalmological features of the ACO2, AFG3L2, and OPA1 groups are summarized in Table 2.

In the ACO2 group, 2 eyes were excluded from analysis because of severe amblyopia and retinal venous occlusion, respectively. Comparable OCT results (DRI Triton, Topcon) were available for 34 of 44 eyes in the ACO2 group, 14 of 26 eyes in the AFG3L2 group, and all 144 eyes in the OPA1 group. VFs were available or comparable (Humphrey, protocol 30-2) for 35 eyes in the ACO2 group, 24 eyes in the AFG3L2 group, and 104 eyes in the OPA1 group.

At fundus examination, the majority of ACO2, OPA1, and AFG3L2 patients presented with temporal (57%, 83%, and 92%, respectively) optic disc pallor (Table 2).

Mean visual acuity in logMAR was 0.41 ± 0.52 in OPA1, 0.39 ± 0.71 in ACO2, and 0.48 ± 0.34 in AFG3L2 groups, with no significant differences between groups

(Table 2). VFs showed a variable degree and pattern of bilateral central scotoma in all patients; however, both MD and fovea sensitivity values did not differ between groups (Table 2). The average RNFL thickness at OCT was 63.62 ± 14.66 in OPA1, 69.28 ± 18.8 in ACO2, and 56.57 ± 14.91 in AFG3L2, without significant differences between groups (Table 2) (Supplemental Figure 1, A). ACO2 patients compared to AFG3L2 patients resulted with higher values in OHN size (P = .020), nasal RNFL thickness (P = .029) (Supplemental Figure 1, D), and average (P = .012), supero-nasal (P = .013), superior (P = .003), inferior (P = .012), and infero-nasal (P = .010) GCL thickness (Supplemental Figure 1, F-L); after adjusting P values for multiple comparisons, significance was confirmed only for the superior sector of the GCL (adjusted P = .026). Comparing ACO2 vs OPA1, ACO2 patients had significantly higher RNFL thickness in the nasal sector (P = .023) (Supplemental Figure 1, D) and higher GCL thickness (Supplemental Figure 1, F-L), both average (P = .0007) and sectorial (supero-nasal P = .027, superior P = .001, supero-temporal P = .003, infero-temporal P = .0005, inferior P = .0001, and infero-nasal P = .004). After adjustment, significance was lost for nasal RNFL, whereas it remained for GCL thickness in average (adjusted P [P<sub>adj</sub>] = .011) and all sectors except the supero-nasal (superior P<sub>adj</sub> = .015, supero-temporal P<sub>adj</sub> = .026, infero-temporal P<sub>adj</sub> = .011, inferior P<sub>adj</sub> = .007, infero-nasal P<sub>adj</sub> = .026) (Supplemental Figure

TABLE 2. Neuro-ophthalmological Results in All ACO2, AFG3L2, and OPA1 Patients

	ACO2	AFG3L2	OPA1	P Value <sup>a</sup>		
				ACO2 vs AFG3L2	ACO2 vs OPA1	OPA1 vs AFG3L2
Eyes, n	44	26	144			
Fundus, n (%)						
Normal	6 (14%)	2 (8%)	2 (1%)			
Temporal pallor	25 (57%)	24 (92%)	120 (83%)			
Diffuse pallor	13 (29%)	0	22 (15%)			
VA, logMAR, mean ± SD	0.39 ± 0.71	0.48 ± 0.34	0.41 ± 0.52	.8246	.9167	.6771
Colors, median (min-max)	1 (0-12)	1 (0.25-3)	2 (0-11)	.5758	.5526	.6222
VF, eyes, n	35	24	104			
MD, dB, mean ± SD	-5.71 ± 4.09	-8.71 ± 7.25	-6.69 ± 4.91	.2870	.4145	.5621
Fovea, dB, mean ± SD	26.84 ± 6.24	26.5 ± 12.26	27.32 ± 9.47	.2391	.1997	.6594
OCT, eyes, n	34	14	144			
OHN area, mm, mean ± SD	2.02 ± 0.43	1.69 ± 0.28	1.86 ± 0.38	.0196*	.2013	.1272
RNFL AVG, μm, mean ± SD	69.28 ± 18.8	56.57 ± 14.91	63.62 ± 14.66	.1134	.3975	.1762
RNFL T, μm, mean ± SD	35.83 ± 13.56	29.86 ± 6.84	32.76 ± 9.64	.2753	.7252	.3684
RNFL S, μm, mean ± SD	91.86 ± 22.6	76.29 ± 25.13	88.09 ± 23.45	.1328	.7195	.2070
RNFL N, μm, mean ± SD	69.41 ± 17.8	51.5 ± 12.33	58.15 ± 13.78	.0287*	.0232*	.2289
RNFL I, μm, mean ± SD	79.80 ± 26.03	69.21 ± 23.1	75.56 ± 21.28	.2221	.6597	.3098
GCL AVG, μm, mean ± SD	49.07 ± 8.98	39.12 ± 8.32	41.84 ± 6.44	.0124*	.0007***	.3656
GCL SN, μm, mean ± SD	49.03 ± 10.78	35.86 ± 9.82	42.54 ± 8.38	.0127*	.0274*	.0566
GCL S, μm, mean ± SD	51.72 ± 9.2	39.5 ± 8.13	44.01 ± 7.88	.0035**	.0012**	.0945
GCL ST, μm, mean ± SD	48.91 ± 9.04	42.00 ± 9.41	41.70 ± 7.45	.2136	.0028**	.9135
GCL IT, μm, mean ± SD	48.03 ± 8.67	42.00 ± 9.21	40.40 ± 6.45	.1832	.0005***	.6172
GCL I, μm, mean ± SD	48.49 ± 7.71	39.07 ± 8.05	41.39 ± 5.26	.0121*	.0001***	.4750
GCL IN, μm, mean ± SD	48.23 ± 10	36.29 ± 8.82	40.91 ± 7.75	.0099**	.0036**	.1829

AVG = average; GCL = ganglion cell layer; I = inferior; IN = infero-nasal; IT = infero-temporal; n = absolute frequency; MD = mean deviation; N = nasal; OCT = optical coherence tomography; ONH = optic nerve head; RNFL = retinal nerve fiber layer; S = superior; SN = supero-nasal; ST = supero-temporal; T = temporal; VA = visual acuity; VF = visual fields.

<sup>a</sup>P value based on Wilcoxon rank sum test using the Rosner–Glynn–Lee method. \*P < .05, \*\* P < .01, \*\*\* P < .001.

Continuous variables are presented as mean ± SD, whereas categorical variables are presented as absolute and relative frequencies.

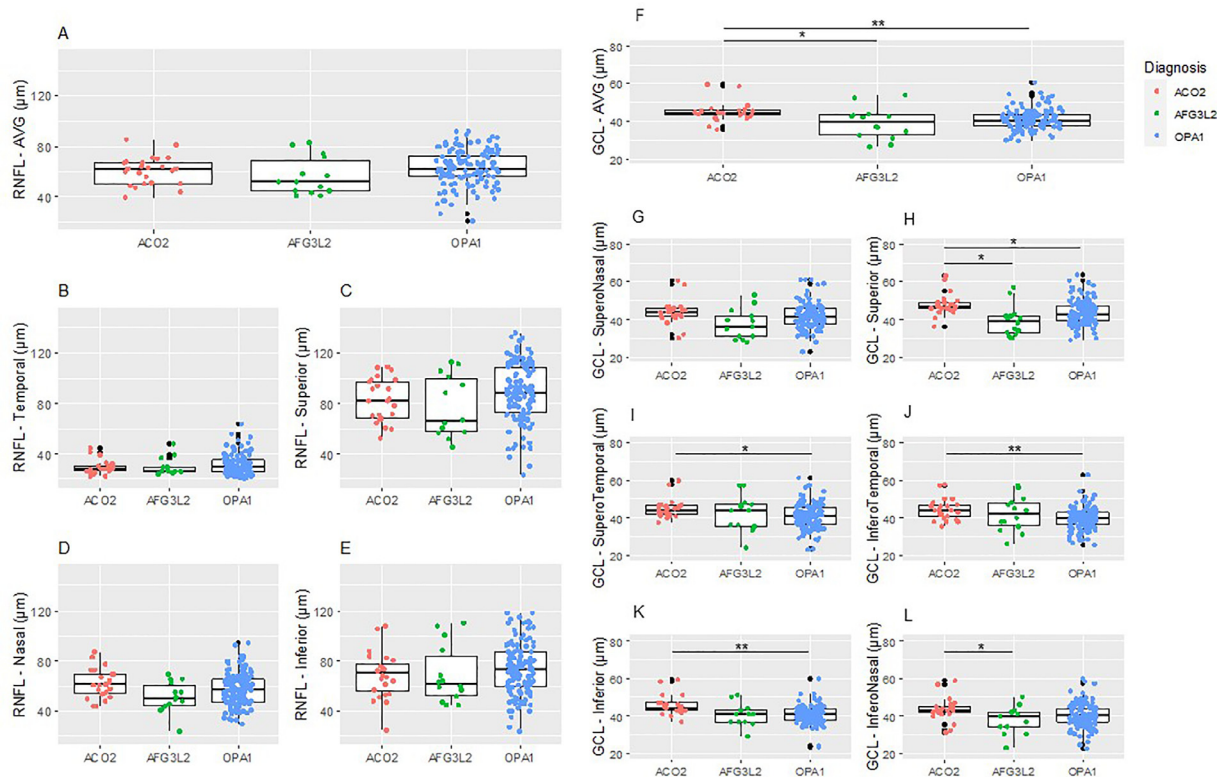


**FIGURE 1.** Average and sectorial retinal nerve fiber layer (RNFL) thickness (A-E) and ganglion cell layer (GCL) thickness (F-L) in ACO2, AFG3L2, and OPA1 symptomatic patients. \* $P < .05$ , \*\* $P < .01$ .

1, F-L). Between the AFG3L2 and OPA1 groups, we found no significant differences in visual and OCT parameters (Table 2).

We thus considered only those patients with reduced visual acuity (affected/symptomatic). Data from 17 ACO2, 11 AFG3L2, and 63 OPA1 were compared (Supplemental Table 3). ACO2 patients compared to AFG3L2 patients had higher values for ONH size ( $P = .044$ ), and average ( $P = .048$ ), superior ( $P = .012$ ), and infero-nasal ( $P = .042$ ) CGL thickness (Figure 1, F-L), whereas compared to OPA1, ACO2 patients had significantly higher GCL thickness on average ( $P = .009$ ), superior ( $P = .015$ ), supero-temporal ( $P = .038$ ), infero-temporal ( $P = .006$ ), and inferior ( $P = .002$ ) sectors (Figure 1, F-L). Nevertheless, after adjusting  $P$  values for multiple comparisons, significance was lost in all parameters. Comparing AFG3L2 and OPA1 groups, we found no differences in any visual or OCT parameters (Figure 1; Supplemental Table 3).

We then focused on the subclinical patients, defined by maintaining normal vision ( $\log\text{MAR} < 0$ ). We were able to compare the OCT data (RNFL and GCL thickness) from only 5 ACO2 and 9 OPA1 patients because, unfortunately, 1 ACO2 and 2 AFG3L2 subclinical patients did not have comparable OCT data (Figure 2). ACO2 patients compared to OPA1 patients showed higher values in

nasal RNFL thickness ( $P = .038$ ), average ( $P = .036$ ), and all sectors GCL thickness except for the superior (supero-nasal  $P = .047$ , supero-temporal  $P = .036$ , infero-temporal  $P = .039$ , inferior  $P = .042$ , and infero-nasal  $P = .02$ ); after adjusting  $P$  values for multiple comparisons, significance was not confirmed (Figure 2).

We looked at sex difference within each group (ACO2, OPA1, and AFG3L2), and we found no statistically significant difference between male and female patients in regard to the neuro-ophthalmological parameters.

We also stratified neuro-ophthalmological results according to the type of mutation (missense or LoF) in the ACO2 and OPA1 groups to find any specific genotype-phenotype correlation. In the ACO2 group, we compared 13 patients with missense mutations (referred to as ACO2-m) with 10 LoF mutation carriers (referred to as ACO2-LoF). We failed to observe any significant difference in the parameters explored between the 2 groups (data not shown). Nevertheless, we observed that ACO-m group showed lower values of GCL thickness close to the significance threshold in the average ( $P = .059$ ), supero-nasal ( $P = 0.056$ ), and superior ( $P = .055$ ) sectors (Figure 3).

Within the OPA1 group, we compared the results of 14 missense carriers (OPA1-m) and 58 patients with LoF mutations (OPA1-LoF). As already described by Barboni *et al*,<sup>30</sup> the OPA1-m group presented with a more severe man-

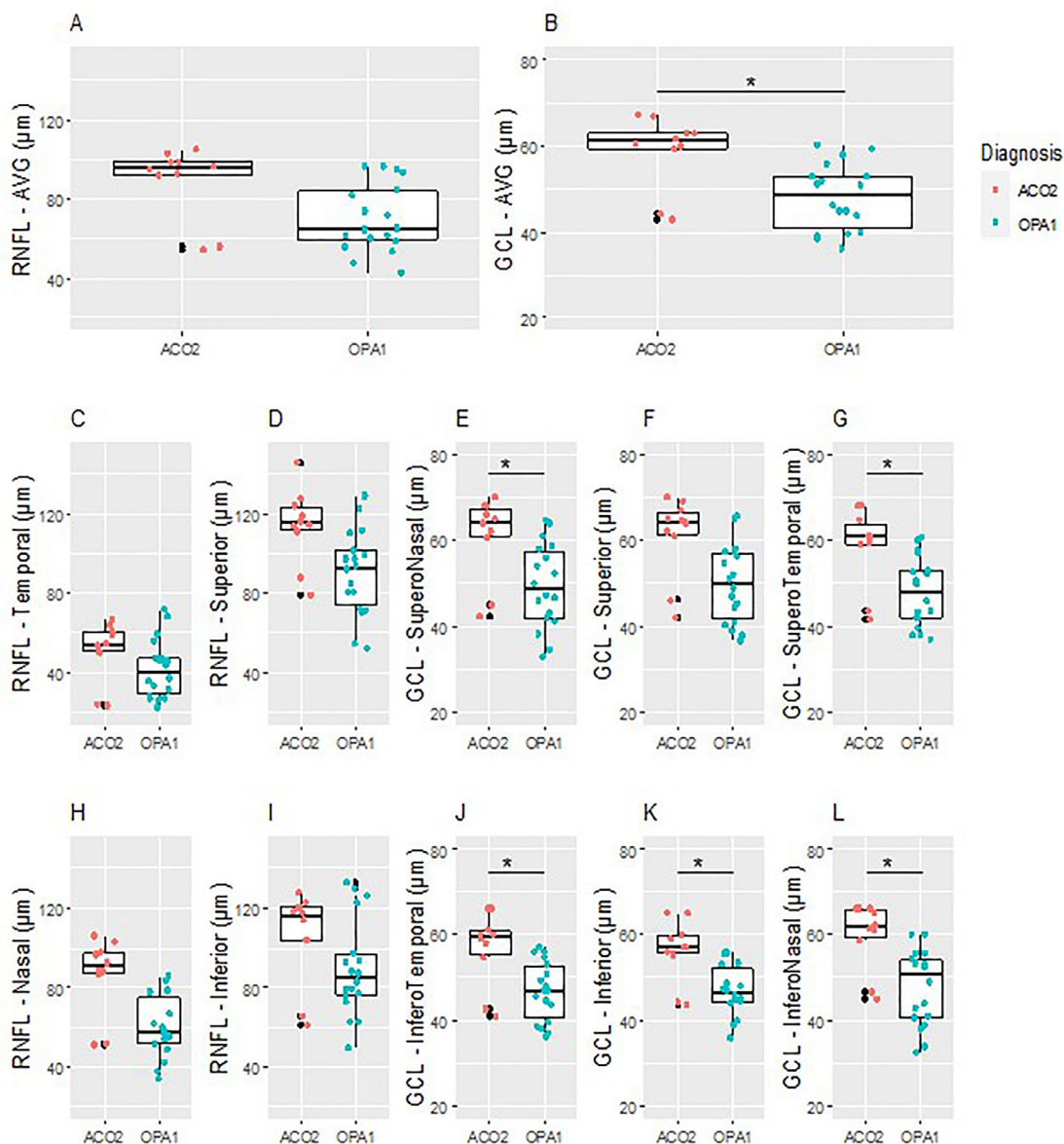


FIGURE 2. Average and sectorial retinal nerve fiber layer (RNFL) and ganglion cell layer (GCL) thickness in ACO2 and OPA1 subclinical patients. \* $P < .05$ .

ifestation of disease, showing lower values of VA ( $P = .01$ ), color vision ( $P = .008$ ), VF mean deviation ( $P = .048$ ), ONH size ( $P = .040$ ), average ( $P = .037$ ), and superior ( $P = .011$ ) RNFL thickness (Supplemental Table 4).

## DISCUSSION

We compared the ophthalmological phenotype of patients carrying two recently defined relatively frequent genetic causes of DOA, namely, ACO2 and AFG3L2 heterozy-

gous mutations,<sup>31</sup> with a matched group of classical OPA1-related DOA patients. We found that, whereas AFG3L2-mutant patients were virtually identical to OPA1-related DOA patients, those carrying monoallelic ACO2 variants had, in general, better RGC preservation, as assessed by RNFL/GCL thickness on OCT, even if visual acuities and visual fields were comparable. This was true for symptomatic patients, but the same pattern was also reflected in the subclinical mutation carriers, in whom an abnormality only on OCT could be detected in the absence of visual defects. The limited case series hampered significance once cases were stratified by mutation category, missense vs LoF

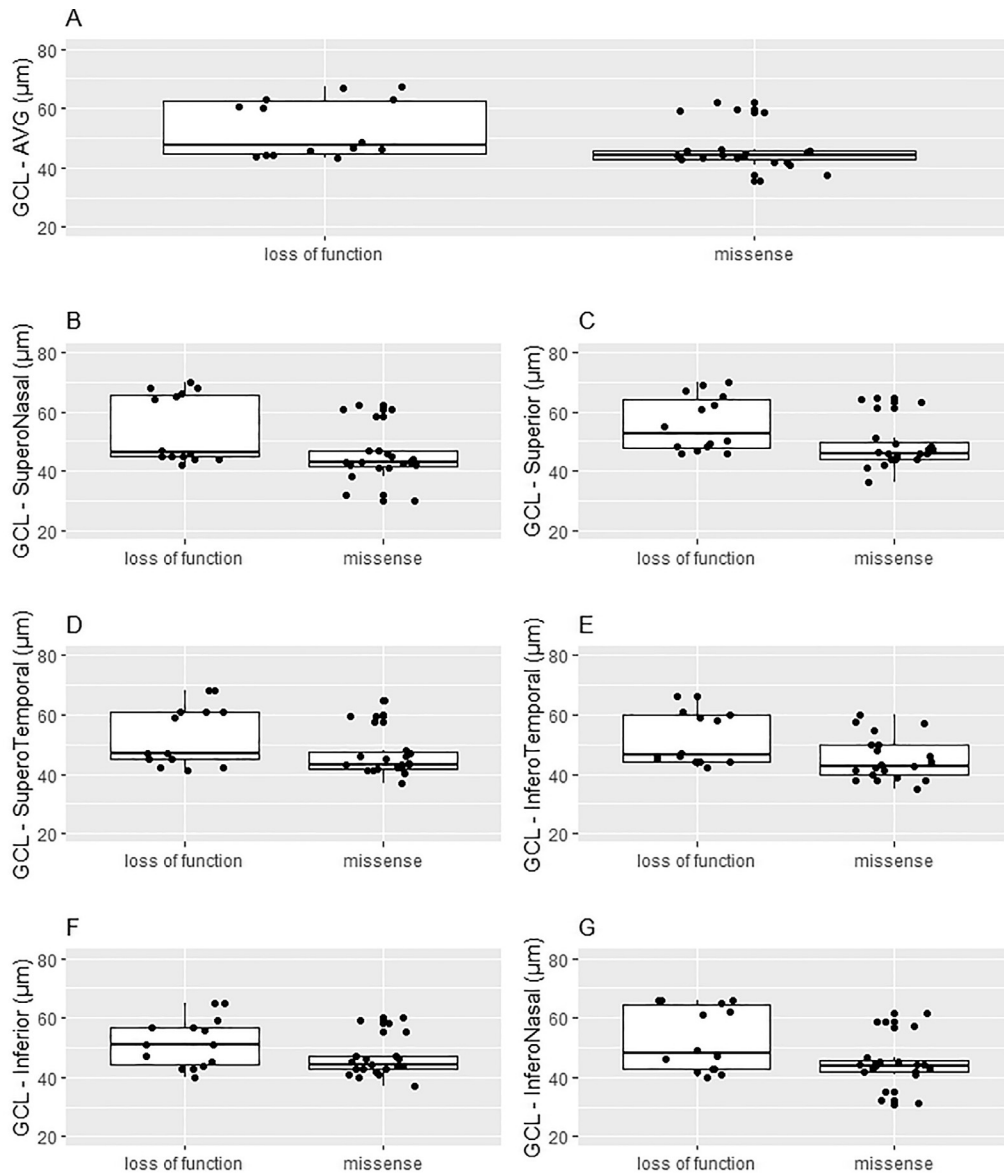


**FIGURE 3.** Average and sectorial ganglion cell layer (GCL) thickness within the ACO2 group, stratified by mutation type: missense or loss of function.

mutations; however, for the well-established greater severity of missense mutations in *OPA1*,<sup>30</sup> a similar tendency was recognized for ACO2. In general, optic atrophy in ACO2 and AFG3L2 patients was congruent with the canonical phenotypic characteristics of *OPA1*-DOA, with a prevalent childhood onset, temporal pallor, and an insidious, stable, or slowly progressive clinical course. Of interest, a higher occurrence of extraocular symptoms was found in AFG3L2 patients, at rates similar to those in the *OPA1* group but different from the ACO2 group, underscoring the close similarity between AFG3L2 and *OPA1*-associated DOA.

The fact that AFG3L2-DOA cases, all carrying missense mutations affecting the ATPase domain, turned out to be

phenocopies of *OPA1*-DOA may be explained by an indirect effect of AFG3L2 mutations on *OPA1* processing. In fact, AFG3L2 encodes a subunit of a proteolytic complex located in the IMM, involved in mitochondrial protein quality control. Mutations affecting the ATPase domain impair both the proteolytic and the dislocase activity of AFG3L2, which is essential for the processing of proteins. The impairment in m-AAA function has been proposed to cause an excess of proteins in the IMM, determining a reduction in mitochondrial membrane potential and activation of the stress-related protease OMA1, which directly processes the long *OPA1* isoforms into shorter ones.<sup>22</sup> We recently demonstrated, in patient-derived fi-



broblasts, that AFG3L2 dysfunction results in the accumulation of short forms of OPA1 reflecting an augmented fragmentation of the mitochondrial network, which is a well-known pathogenic paradigm for mitochondrial optic neuropathies.<sup>12</sup> Hence, the mechanism by which AFG3L2 mutations lead to optic atrophy is assumed to be the unbalanced processing of OPA1, ultimately causing a phenotype that is indistinguishable from OPA1-related DOA. The same mechanism is proposed for DOA associated with dominant mutations in SPG7 gene, the protein product of which combines with AFG3L2 to form the m-AAA protease and the recessive mutations of which cause hereditary spastic paraplegia type 7 (HSP7).<sup>23</sup> Notably, in contrast to AFG3L2 DOA-associated mutations, the SPG7 variants leading to DOA seem to be dispersed among the recessive variants that cause HSP7. Moreover, mutations leading to frameshift suggest that SPG7 haploinsufficiency might be the primary pathophysiologic mechanism determining DOA.<sup>13</sup>

On the other hand, ACO2-DOA, despite being no different in terms of functional measures such as VA and VF parameters, consistently showed higher values of nasal RNFL and GCL thickness compared to both AFG3L2 and OPA1 patients. The reason for this anatomical difference, which was confirmed also in subclinical patients, might be a different pathogenic mechanism not involving OPA1. ACO2 seems to play a role, regardless its enzymatic activity in the Krebs cycle, also in mtDNA maintenance. In fact, studies on fibroblasts with ACO2 mutations have shown, in conjunction with reduced levels of the protein, a reduction of mtDNA copy number up to 50%, which caused impaired mitochondrial respiration and increased susceptibility to stress-induced and metabolically demanding conditions.<sup>27</sup> This could eventually be the cause of the optic nerve atrophy observed in heterozygous ACO2 mutations. Interestingly, a similar mechanism has been described in fibroblasts derived from patients with mutations, either dominant or recessive, in another nuclear gene, the single-stranded binding protein 1 (SSBP1). This gene encodes for a key factor of the mtDNA replisome.<sup>32</sup> SSBP1 mutations, as for ACO2, can be transmitted as autosomal dominant or recessive traits and can lead to either isolated optic atrophy, as in our ACO2 patients, or a complex syndromic form including retinal macular dystrophy, sensorineural deafness, myopathy, and kidney dysfunction. The mechanism by which SSBP1 mutations cause pathology is now established to depend on impaired mtDNA replication, which in turn leads to mtDNA depletion without accumulation of multiple deletions.<sup>15-17</sup> As a final note, both ACO2 and SSBP1 genes on the severe end of the clinical spectrum may also affect the retinal pigment epithelium and photoreceptors, in addition to the RGCs

and optic nerve, as mtDNA partial depletion in the retina may affect all energy-dependent cell types.<sup>33</sup>

Concerning the genotype–phenotype correlations, we confirmed once again that OPA1 missense mutations displayed a more severe phenotype compared to LoF mutations, both in terms of functional and anatomical parameters.<sup>30,34</sup> In the current study, a similar tendency, albeit not statistically significant given the small cohort, was observed with ACO2-DOA patients. Patients harboring a missense mutation showed overall lower values of VA, VF, and OCT parameters, especially in the GCL, compared to patients with a mutation predicted to cause LoF. We can postulate a similar dominant negative mechanism for missense mutation in ACO2, as described for OPA1. However, it must be noted as a limitation that formal demonstration of the genetic mechanism consequent to the pathogenic variants was available only for some, and to solidly define the genotype–phenotype correlation, an effort to mechanistically define the ultimate effect of each variant, including the missense mutations, should be made for each gene studied.

The main limitation of the current study is the exploratory and retrospective nature of our investigation, in a limited number of cases, in particular considering the AFG3L2 patients, which meant that some of the eyes lacked some neuro-ophthalmological assessments. ACO2 has recently been ranked as the third most frequent gene causing inherited optic neuropathy,<sup>31,35</sup> and we envisage that larger datasets will be available to replicate the current observations.

Moreover, we noticed a significant sex skew toward male patients in the AFG3L2 and ACO2 patients (~70%), which we consider at this stage to likely be due to chance, given the small size of the cohorts, affecting the corresponding sex-matched skew in the OPA1 cohort. Although in OPA1-associated DOA there is no clear evidence of sex bias,<sup>36</sup> this remains poorly investigated in other, rarer inherited optic neuropathies such as AFG3L2 and ACO2-related DOA. Nevertheless, we failed to observe any significant difference in neuro-ophthalmological features between male and female patients.

In conclusion, DOA remains a homogeneous entity on clinical grounds, despite the growing genetic heterogeneity underlying the disease. However, ACO2 seems to stand out for being an overall milder phenotype, in terms of better preservation of RGCs; we propose that this might depend on a different pathogenic mechanism involving mtDNA maintenance as opposed to AFG3L2, which follows the OPA1 dysfunction paradigm. These differences may be reflected in the future in terms of a better prognosis for ACO2, once therapeutic approaches are available.

---

## CREDIT AUTHORSHIP CONTRIBUTION STATEMENT

**Giulia Amore:** Conceptualization, Data curation, Formal analysis, Investigation, Project administration, Writing – original draft, Writing – review & editing, Methodology, Validation. **Martina Romagnoli:** Conceptualization, Data curation, Formal analysis, Methodology, Software, Writing – original draft, Writing – review & editing. **Michele Carbonelli:** Data curation, Investigation, Methodology, Software, Validation, Visualization, Writing – original draft, Writing – review & editing. **Maria Lucia Casavilla:** Data curation, Investigation, Validation, Writing – original draft, Writing – review & editing. **Anna Maria De Negri:** Data curation, Investigation, Validation, Writing – original draft, Writing – review & editing. **Arturo Carta:** Data curation, Investigation, Validation, Writing – original draft, Writing – review & editing. **Vincenzo Parisi:** Data curation, Funding acquisition, Investigation, Resources, Validation, Writing – original draft, Writing – review & editing. **Antonio Di Renzo:** Data curation, Formal analysis, Methodology, Software, Writing – original draft, Writing – review & editing. **Costantino Schiavi:** Data curation, Investigation, Validation, Writing – orig-

inal draft, Writing – review & editing. **Chiara Lenzetti:** Data curation, Investigation, Validation, Writing – original draft, Writing – review & editing. **Corrado Zenesini:** Conceptualization, Data curation, Formal analysis, Methodology, Software, Validation, Writing – original draft, Writing – review & editing. **Danara Ormanbekova:** Data curation, Formal analysis, Investigation, Methodology, Software, Writing – original draft, Writing – review & editing. **Flavia Palombo:** Data curation, Formal analysis, Investigation, Methodology, Software, Validation, Writing – original draft, Writing – review & editing. **Claudio Fiorini:** Data curation, Formal analysis, Investigation, Methodology, Software, Validation, Writing – original draft, Writing – review & editing. **Leonardo Caporali:** Conceptualization, Data curation, Formal analysis, Funding acquisition, Investigation, Methodology, Software, Supervision, Validation, Writing – original draft, Writing – review & editing. **Valerio Carelli:** Conceptualization, Funding acquisition, Methodology, Project administration, Resources, Supervision, Validation, Visualization, Writing – original draft, Writing – review & editing. **Piero Barboni:** Conceptualization, Data curation, Investigation, Methodology, Supervision, Validation, Writing – original draft, Writing – review & editing. **Chiara La Morgia:** Conceptualization, Funding acquisition, Methodology, Project administration, Resources, Supervision, Validation, Visualization, Writing – original draft, Writing – review & editing.

---

Funding/Support: This study was supported by the Italian Ministry of Health with the grant [GR-2016-02361449](#) “Italian Project on Hereditary Optic Neuropathies (IPHON): from genetic basis to therapy” to L.C. and the “Ricerca Corrente” funding to V.C for studies on “Genetic Basis of Inherited Optic Neuropathies” and by Chiesi Pharmaceuticals with the sponsored study “Natural History of Inherited Optic Neuropathies” to V.C. V.P and A.D.R. were supported by the Italian Ministry of Health “Ricerca Corrente” and Fondazione Roma. Financial Disclosures: V.C. and C.L.M. received consultant fees and travel reimbursements from Gensight Biologics and Chiesi Pharmaceuticals; V.C. participated on advisory board in Gensight Biologics and Chiesi Pharmaceuticals; C.L.M. received speaker honoraria from Chiesi Pharmaceuticals, Regulatory Pharmanet, The Newway srl, and Biologix; M.R. received speaker honoraria, consulting fees, and travel reimbursement from Santhera Pharmaceuticals and GenSight Biologics; M.C. received consulting fees from Gensight Biologics and Santhera Pharmaceuticals; V.C., G.A., C.L.M. received speaker honoraria from First Class; V.P. received speaker honoraria from Omikron Italia; P.B. received personal honoraria from Gensight Biologics. None of these activities are related to conducting this study and writing the manuscript. All authors attest that they meet the current ICMJE criteria for authorship.

---

## REFERENCES

1. Lenaers G, Neutzner A, Le Dantec Y, et al. Dominant optic atrophy: culprit mitochondria in the optic nerve. *Prog Retin Eye Res.* 2020;100935. doi:[10.1016/j.preteyeres.2020.100935](#).
2. Yu-Wai-Man P, Griffiths PG, Gorman GS, et al. Multi-system neurological disease is common in patients with OPA1 mutations. *Brain.* 2010;133(Pt 3):771–786. doi:[10.1093/brain/awq007](#).
3. Carelli V, Musumeci O, Caporali L, et al. Syndromic parkinsonism and dementia associated with OPA1 missense mutations. *Ann Neurol.* 2015;78(1):21–38. doi:[10.1002/ana.24410](#).
4. Delettre C, Lenaers G, Griffioen JM, et al. Nuclear gene OPA1, encoding a mitochondrial dynamin-related protein, is mutated in dominant optic atrophy. *Nat Genet.* 2000;26(2):207–210. doi:[10.1038/79936](#).
5. Alexander C, Votruba M, Pesch UE, et al. OPA1, encoding a dynamin-related GTPase, is mutated in autosomal dominant optic atrophy linked to chromosome 3q28. *Nat Genet.* 2000;26(2):211–215. doi:[10.1038/79944](#).
6. Del Dotto V, Fogazza M, Carelli V, Rugolo M, Zanna C. Eight human OPA1 isoforms, long and short: what are they for? *Biochim Biophys Acta Bioenerg.* 2018;1859(4):263–269. doi:[10.1016/j.bbabi.2018.01.005](#).
7. Gerber S, Charif M, Chevrollier A, et al. Mutations in DNMI1, as in OPA1, result in dominant optic atrophy despite opposite effects on mitochondrial fusion and fission. *Brain.* 2017;140(10):2586–2596. doi:[10.1093/brain/awx219](#).
8. Maresca A, Carelli V. Molecular mechanisms behind inherited neurodegeneration of the optic nerve. *Biomolecules.* 2021;11(4):496. doi:[10.3390/biom11040496](#).
9. Newman NJ, Yu-Wai-Man P, Biousse V, Carelli V. Understanding the molecular basis and pathogenesis of hereditary optic neuropathies: towards improved diagnosis and management. *Lancet Neurol.* 2023;22(2):172–188. doi:[10.1016/S1474-4422\(22\)00174-0](#).

10. Charif M, Roubertie A, Salime S, et al. A novel mutation of AFG3L2 might cause dominant optic atrophy in patients with mild intellectual disability. *Front Genet.* 2015;6:311. doi:10.3389/fgene.2015.00311.
11. Colavito D, Maritan V, Suppiej A, et al. Non-syndromic isolated dominant optic atrophy caused by the p.R468C mutation in the AFG3 like matrix AAA peptidase subunit 2 gene. *Biomed Rep.* 2017;7(5):451–454. doi:10.3892/br.2017.987.
12. Caporali L, Magri S, Legati A, et al. ATPase domain AFG3L2 mutations alter OPA1 processing and cause optic neuropathy. *Ann Neurol.* 2020;88(1):18–32. doi:10.1002/ana.25723.
13. Charif M, Chevrollier A, Gueguen N, et al. Mutations in the m-AAA proteases AFG3L2 and SPG7 are causing isolated dominant optic atrophy. *Neurol Genet.* 2020;6(3):e428. doi:10.1212/NXG.0000000000000428.
14. Charif M, Gueguen N, Ferré M, et al. Dominant ACO2 mutations are a frequent cause of isolated optic atrophy. *Brain Commun.* 2021;3(2):fcab063. doi:10.1093/braincomms/fcab063.
15. Jurkute N, Leu C, Pogoda HM, et al. SSBP1 mutations in dominant optic atrophy with variable retinal degeneration. *Ann Neurol.* 2019;86(3):368–383. doi:10.1002/ana.25550.
16. Piro-Mégy C, Sarzi E, Tarrés-Solé A, et al. Dominant mutations in mtDNA maintenance gene SSBP1 cause optic atrophy and foveopathy. *J Clin Invest.* 2020;130(1):143–156. doi:10.1172/JCI128513.
17. Del Dotto V, Ullah F, Di Meo I, et al. SSBP1 mutations cause mtDNA depletion underlying a complex optic atrophy disorder. *J Clin Invest.* 2020;130(1):108–125. doi:10.1172/JCI128514.
18. Courage C, Jackson CB, Hahn D, et al. SDHA mutation with dominant transmission results in complex II deficiency with ocular, cardiac, and neurologic involvement. *Am J Med Genet A.* 2017;173(1):225–230. doi:10.1002/ajmg.a.37986.
19. Gerdes F, Tatsuta T, Langer T. Mitochondrial AAA proteases—towards a molecular understanding of membrane-bound proteolytic machines. *Biochim Biophys Acta.* 2012;1823(1):49–55. doi:10.1016/j.bbamcr.2011.09.015.
20. Di Bella D, Lazzaro F, Brusco A, et al. Mutations in the mitochondrial protease gene AFG3L2 cause dominant hereditary ataxia SCA28. *Nat Genet.* 2010;42(4):313–321. doi:10.1038/ng.544.
21. Pierson TM, Adams D, Bonn F, et al. Whole-exome sequencing identifies homozygous AFG3L2 mutations in a spastic ataxia-neuropathy syndrome linked to mitochondrial m-AAA proteases. *PLoS Genet.* 2011;7(10):e1002325. doi:10.1371/journal.pgen.1002325.
22. Baderna V, Schultz J, Kearns LS, et al. A novel AFG3L2 mutation close to AAA domain leads to aberrant OMA1 and OPA1 processing in a family with optic atrophy. *Acta Neuropathol Commun.* 2020;8(1):93. doi:10.1186/s40478-020-00975-w.
23. Casari G, De Fusco M, Ciarmatori S, et al. Spastic paraplegia and OXPHOS impairment caused by mutations in paraplegin, a nuclear-encoded mitochondrial metalloprotease. *Cell.* 1998;93(6):973–983.
24. Klebe S, Depienne C, Gerber S, et al. Spastic paraplegia gene 7 in patients with spasticity and/or optic neuropathy. *Brain.* 2012;135(Pt 10):2980–2993.
25. Metodiev MD, Gerber S, Hubert L, et al. Mutations in the tricarboxylic acid cycle enzyme, aconitase 2, cause either isolated or syndromic optic neuropathy with encephalopathy and cerebellar atrophy. *J Med Genet.* 2014;51(12):834–838. doi:10.1136/jmedgenet-2014-102532.
26. Spiegel R, Pines O, Ta-Shma A, et al. Infantile cerebellar-retinal degeneration associated with a mutation in mitochondrial aconitase, ACO2. *Am J Hum Genet.* 2012;90(3):518–523. doi:10.1016/j.ajhg.2012.01.009.
27. Neumann MA, Grossmann D, Schimpf-Linzenbold S, et al. Haploinsufficiency due to a novel ACO2 deletion causes mitochondrial dysfunction in fibroblasts from a patient with dominant optic nerve atrophy. *Sci Rep.* 2020;10(1):16736. doi:10.1038/s41598-020-73557-4.
28. Barboni P, Savini G, Valentino ML, et al. Retinal nerve fiber layer evaluation by optical coherence tomography in Leber's hereditary optic neuropathy. *Ophthalmology.* 2005;112(1):120–126. doi:10.1016/j.ophtha.2004.06.034.
29. Benjamini Y, Yekutieli D. The control of the false discovery rate in multiple testing under dependency. *Ann Stat.* 2001;29:1165–1188.
30. Barboni P, Savini G, Cascavilla ML, et al. Early macular retinal ganglion cell loss in dominant optic atrophy: genotype-phenotype correlation. *Am J Ophthalmol.* 2014;158(3):628–636. doi:10.1016/j.ajo.2014.05.034.
31. Rocatcher A, Desquret-Dumas V, Charif M, et al. The top 10 most frequently involved genes in hereditary optic neuropathies in 2186 probands. *Brain.* 2022:awac395. doi:10.1093/brain/awac395.
32. Jiang M, Xie X, Zhu X, et al. The mitochondrial single-stranded DNA binding protein is essential for initiation of mtDNA replication. *Sci Adv.* 2021;7(27):eabf8631. doi:10.1126/sciadv.abf8631.
33. Zeviani M, Carelli V. Mitochondrial retinopathies. *Int J Mol Sci.* 2021;23(1):210. doi:10.3390/ijms23010210.
34. Yu-Wai-Man P, Griffiths PG, Burke A, et al. The prevalence and natural history of dominant optic atrophy due to OPA1 mutations. *Ophthalmology.* 2010;117:1538–1546.
35. Fiorini C, Ormanbekova D, Palombo F, et al. The Italian reappraisal on the most frequent genetic defects in hereditary optic neuropathies and the global top 10. *Brain.* 2023:awad080. doi:10.1093/brain/awad080.
36. Lenaers G, Neutner A, Le Dantec Y, et al. Dominant optic atrophy: culprit mitochondria in the optic nerve. *Prog Retin Eye Res.* 2021;83:100935. doi:10.1016/j.preteyeres.2020.100935.